

Modeling of Flow Passing Backward Facing Step

Mohamed Milad Ahmed*

Department of Petroleum, Faculty of Engineering, Sirte University, Sirte, Libya
E-mail: massiwi@su.edu.ly

Abstract

Flows passing sudden diameter expansion of ducts can be found in many industrial situations such as flows in annular spaces between drill pipes and open or cased holes while circulating drilling fluids down the wells and up the annular spaces to surface during oil and gas wells drilling. As a first step towards understanding the flow behavior in situation like theses, a simulation of flows similar to this has been carried out. This paper presents results of a computational study of steady, compressible flow over a backward facing-step in a wide, two dimensional duct. The flow in this duct has been investigated experimentally by previous workers [1] and so provides a useful benchmark test case. In the present work the commercial CFD code Fluent v6.0.20 is used to compute results for the range of Reynolds numbers $70 < Re < 7000$, where Re is based on two-thirds of maximum velocity and duct height upstream of the step. This range includes the laminar, transitional and low Reynolds number turbulent flow regimes, for which significant variations in the separation length have been measured. The results to be presented will include the variation of velocity distributions and separation lengths for the recirculating flow region downstream of the step with Reynolds number.

Keywords: Induction machine, diagnostics, current spectrum, harmonics.

Abbreviations and Acronyms

A	Cross-sectional-Area
B	Empirical constant (Law of the Wall)
D	Diameter (mm)
d_e	External diameter of the drill pipe (mm)
E	Empirical constant (Law of the Wall)
$k-\varepsilon$	Turbulence model
$k-\omega$	Turbulence model
Re	Reynolds number
Re_Q	Axial Reynolds Number
r_i	Inner radius (mm)
r_o	Outer radius (mm)
U	x Component of mean flow velocity (m/s)
\bar{U}	Average velocity (m/s)
u^+	Dimensionless velocity

u_i^+	Inner wall dimensionless velocity
u_o^+	Outer wall dimensionless velocity
V	y Component of mean flow velocity (m/s)
y^+	Dimensionless distance from wall
y_i^+	Dimensionless distance from the inner wall
y_o^+	Dimensionless distance from the outer wall
CFD	Computational Fluid Dynamics
UDF	User defined functions
Greek	
ν	Kinematic viscosity (m^2/s)
κ	Von Karman's constant (law of the wall)

1. Introduction

Many studies have been devoted to this issue, eg in two dimensions [1], [2] and [3], and in three dimensions [4], [5], [6] and [7]. Flow through an axisymmetric expansion without inlet swirl has also been studied to focus on the physics of wall-bounded separated reattached flow, eg by [8] and [9].

A further investigation of sudden expansion with inlet swirl was performed by [10]. The simplicity of the geometry, on the one hand, and the intrinsic complexity of the flow field (ie flow separation, reversal and reattachment), on the other hand, have resulted in its acceptance as a benchmark problem for testing computational codes. Flow separation can be defined as a region of recirculating flow adjacent to the solid boundary. The regions for detachment and reattachment of the 'separation bubble' are delimited by contours of zero vorticity near the boundary. Within the separation bubble the flow is characterized by recirculating vortices and flow reversal [6]. Dimensional analysis suggests that any flow variable of interest, for example the reattachment length, is a function of several non-dimensional parameters, most importantly, the expansion ratio, step-height Reynolds number and the non-dimensional upstream boundary-layer thickness and state [11].

The objective of this study is to computationally investigate flow over a 2D backward facing step, using the step geometry and flow conditions reported by. A comparison of computed and experimental results carried out by Armaly et al is to be performed to validate the modeling methods used. An open loop air-driven flow channel was used by [1] to measure

velocity distributions and reattachment lengths downstream of a backward-facing step, Fig 1. Results were presented for laminar, transitional and turbulent flow of air with a Reynolds number range of $70 < Re < 7000$. The channel height upstream of the step, h_1 , was 5.2 mm and the downstream channel height, h_2 , was 10.1 mm , giving an expansion ratio $ER = h_2/h_1 = 1.94$, and step height S of 4.9 mm . The channel width W was 180 mm and $W/S = 36.7$. The test section provided a 200 mm straight channel approach to the backward-facing step and a 500 mm long channel downstream of the step.

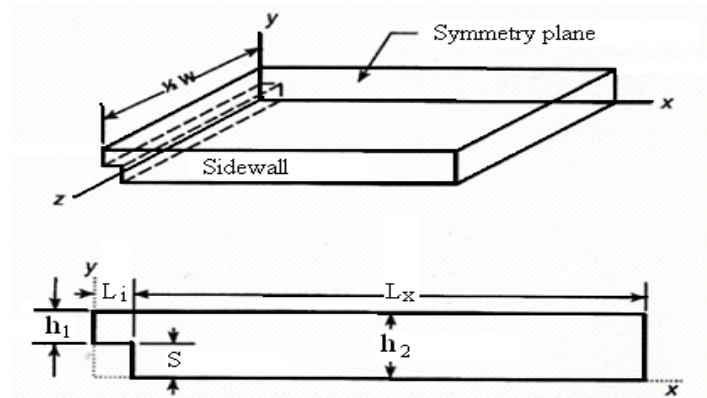


Figure 1. Backward-facing step geometry used by [1].

Laser Doppler measurements of the reattachment length for the primary separation region, X1 in Fig 2, just downstream of the step on the lower wall, allowed the identification of the laminar ($Re < 1200$), transitional ($1200 < Re < 6600$) and turbulent ($Re > 6600$) regions (the Reynolds number is based on velocity equal to two-thirds of the maximum velocity measured 10 mm upstream of the step and a reference length equal to twice the upstream channel height). For the laminar regime, the separation length increases linearly with the Reynolds number. The transitional flow regime is characterized by a sharp initial decrease in the reattachment length, followed by a continued gradual but irregular decrease to a minimum at a Reynolds number of approximately 5500 . Beyond $Re = 6600$ the reattachment length ceases to be a function of Reynolds number, Fig 3. An additional separation region was measured along the floor downstream of the primary separation, X2 and X3 in Fig 2. This secondary separation region

disappears above a Reynolds number of 2300. A secondary separation region was also observed along the upper wall downstream of the step, X4 and X5 in Fig 5.2. It develops in the laminar regime (for $Re > 400$) and remains throughout the transition regime. The length of this upper separation region initially increases with increasing Reynolds number and then gradually decreases until it disappears above a Reynolds number of approximately 6600, Fig 3.

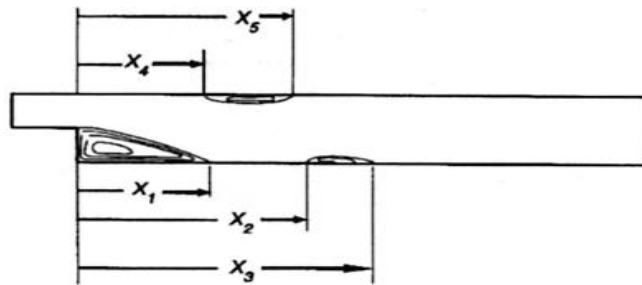


Figure 2. Separation regions identified by [1].

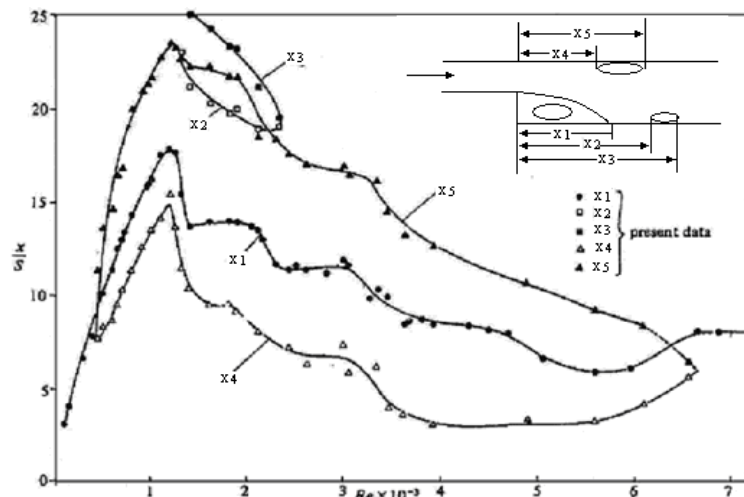


Figure 3. Measured longitudinal dimensions of separated flow regions downstream of backward-facing step; variation of locations with Reynolds number [1].

2. Computational Modeling

The computational boundary conditions, boundary types, Re definition, and expansion ratio $ER = 1.94$ should match those experimentally conducted by [1]. Fig 4 shows the schematic view of the flow domain used in the 2-dimensional simulation. The computation domain consists of a streamwise length $L_x = 90S$ including an inlet section, $L_i = 41S$ prior to the sudden expansion, vertical height $L_y = 2.06S$, where S is the height of the step. The flow geometry was

made up of an inlet duct of 5.2 mm in height expanding into a duct of 10.1 mm height yielding an expansion ratio for $ER = \frac{L_y}{(L_y - S)} = 1.94$. The origin is at the lower end of the step. The

definition of the Reynolds number used in this computational study is given by $Re = \frac{UD}{\nu}$, where U is the two-thirds of the measured maximum velocity at a distance $L_i = -2S$, D is the hydraulic diameter of (small) channel and equivalent to twice its height ($D = 2 h_1$), and ν is the kinematic viscosity of the working fluid.

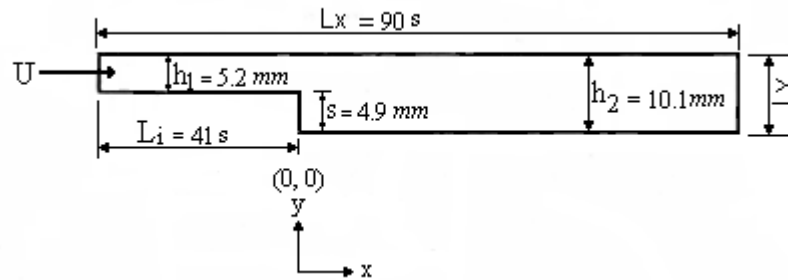


Figure 4. Computational model geometry.

The section lengths downstream of the step and prior to the step were sufficiently long to permit the flow to be developed into a fully developed channel flow, i.e. $\frac{\partial U}{\partial x} = 0$.

Fig 5 and 6 show developed flows prior to the step and prior to the exit, respectively. To check the inlet length three tests were applied:

- the computational inlet was doubled, and
- both uniform and parabolic velocity profiles were used for the specified inlet velocity conditions, for both RSM and $k-\epsilon$ turbulence closures, but none of these influence the profile shown in Fig 5

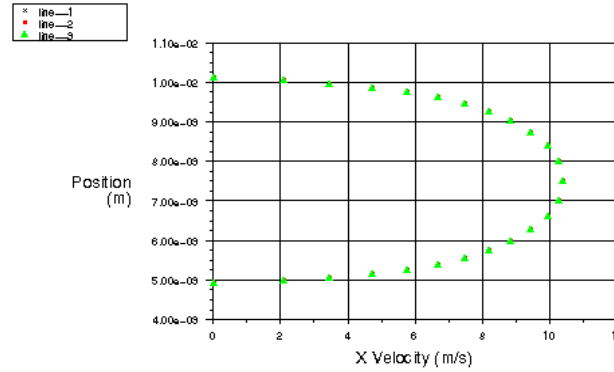


Figure 5. Developed flow prior to the step (RSM modeling method), $Re = 6000$.

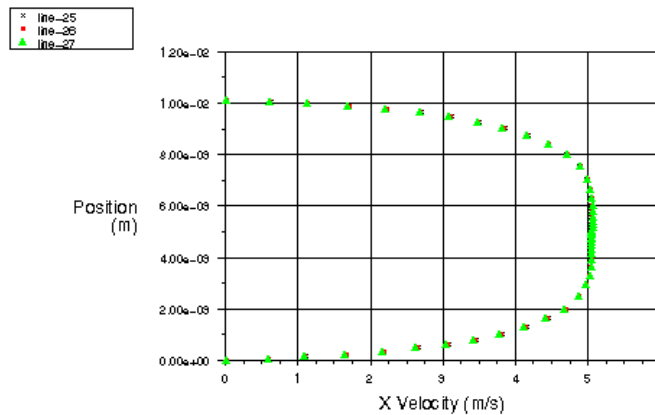


Figure 6. Developed flow prior to the exit (RSM modeling method), $Re = 6000$.

Fig 7 gives the boundary conditions applied in this computation. They consisted of zero slip boundary conditions at the walls ($u, v = 0$). The wall function treatment was set to enhanced wall treatment. To ensure the validity of the wall function treatment the y^+ value of the near wall nodes was verified after simulations around one. Also, it was confirmed that the number of cells in the viscosity effected near wall region ($Re_y < 200$) met the minimum required of ten cells [12] (Fluent Inc 2001 p.10-78). Gauge pressure was set to zero at the outlet. The specified inlet velocity at $x = -41S$ upstream of the step was without any cross-stream component ($u = \text{constant}$ and $v = 0$). The velocity profile prior to the step and exit of the computational domain was assumed to be fully developed. Thus, the streamwise derivative of the velocity component is zero.

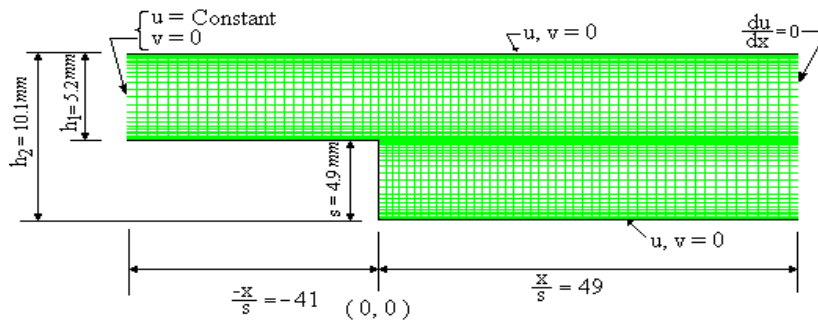


Figure 7. Solution domain and boundary conditions.

3. Flow Computation and Results

To carry out grid dependence investigations of the flow computations, several numerical meshes were considered. as a result of these, the grid chosen for obtaining the results presented is 240*24 above the step height and 200*24 below the step height. To precisely examine the flow near the step and the walls, the distribution of the grid nodes was non-uniform in both coordinate directions allowing higher grid node concentrations in the region close to the step, along the shear region and close to both walls of the duct upstream and downstream of the step.

- **Effect of Reynolds Numbers on Circulation Region Lengths:**

The reattachment length $X1$ at the bottom wall of the model is the main feature of the recirculation flow structure downstream of the backward facing step, as it lasts throughout the whole range of Reynolds numbers used, whereas the other two circulation separation regions at the top and bottom walls appear and disappear at certain ranges of Reynolds numbers.

Computational model for laminar flow, Lam-Premhorst and Launder-Sharma Models for low turbulent Reynolds Numbers, and turbulent models (RNG $k-\epsilon$, $k-\omega$ and RSM) were used for this simulation study. Reattachment length $X1$ in particular was examined over the whole range of Reynolds numbers. Fig 8 and 9 show velocity contours and velocity profiles of the main circulation region respectively. Fig 9 shows a circulation flow just next to the step with a reverse flow at the bottom of the axial velocity profile. Computational results obtained by

Fluent for predicting steady separated flows for the whole range of Reynolds numbers are shown in Fig 10 through 18.

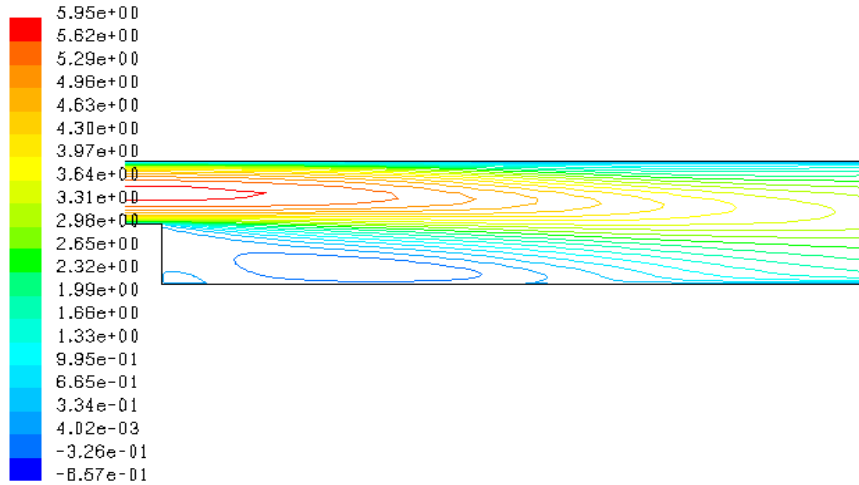


Figure 8. Velocity contours of first circulation region for a typical Reynolds number 3250 (RSM modeling method).

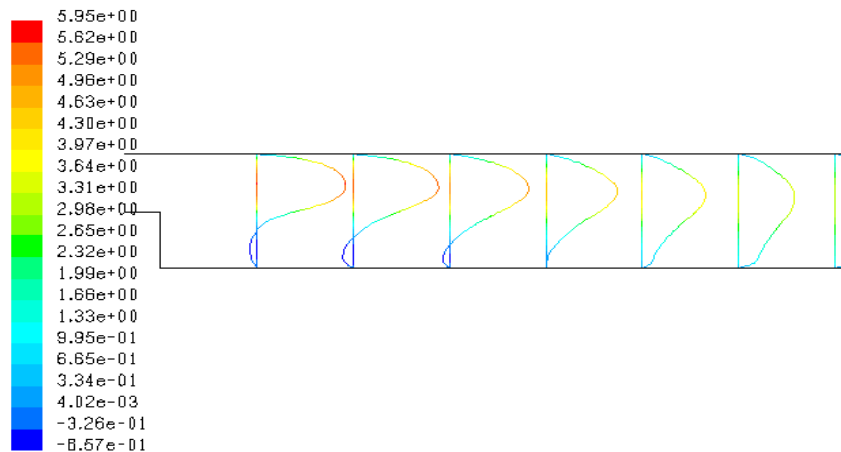


Figure 9. Axial velocity profile for a typical Reynolds number 3250 (RSM Modeling Method).

Low laminar Reynolds numbers <1000 were investigated by the laminar modeling method only. Fig 10 shows a comparison between computed and experimental results. A fairly good agreement was obtained between experimental and computational results for Reynolds numbers $Re < 400$, with disagreement between computed and measured results after $Re = 400$ where the results started to diverge. The increased disagreement between experimental and 2-

dimensional computational results at higher Reynolds numbers > 400 is caused by the occurrence of inherent three-dimensional flow effects[2].

The range of Reynolds numbers between 1000 and 7000 was investigated by the various different modeling methods used. Fig 11 shows a comparison between the laminar flow modeling method and experimental results. Reasonable agreement is obtained, with both sets of results showing that the reattachment length is decreasing with Reynolds number. Results obtained by using the low Reynolds modeling methods of Lam-Premhorst and Launder-Sharma are displayed in Fig 12 and 13. These show disagreement between computed and measured results. Fig 12 shows that the reattachment length is decreasing with Reynolds number in both cases, but with a big difference in values between computed and measured, where the computed separation length is much less than the measured results. In contrast, computed separation length by the Launder-Sharma modeling method shows that the reattachment length is constant with a value of X/S about 5.2 with increasing Reynolds numbers, with some errant values of separation length for Reynolds numbers between 3000 and 5000 as shown in Fig 13.

Comparison between experimental and computed results obtained by turbulent modeling is shown in Fig 14 through 18. There is disagreement between experimental and computational results for all of the modeling methods used, and they even contradict each other. Where RNG $k-\varepsilon$ modeling method shows that the separation length gradually increases with Reynolds number, RSM shows the separation length is constant, whereas $k-\omega$ with its variants shows the separation length gradually increases with Reynolds number by values much higher than with the RNG $k-\varepsilon$ modeling method.

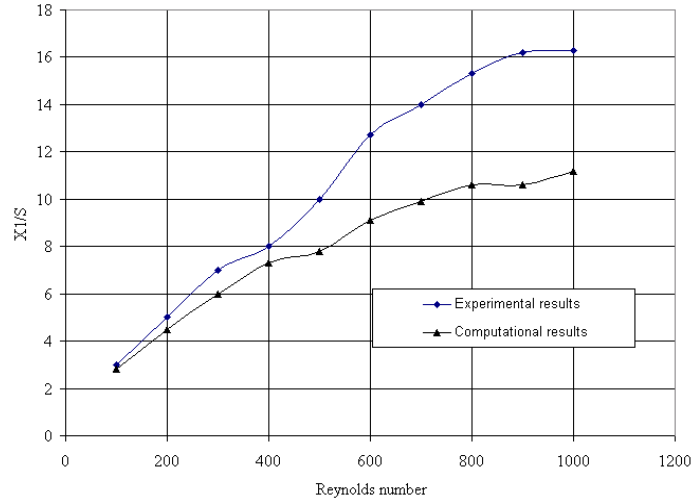


Figure 10. Comparison of experimental and computational X_1 reattachment length for $Re < 1000$ (laminar flow modeling method).

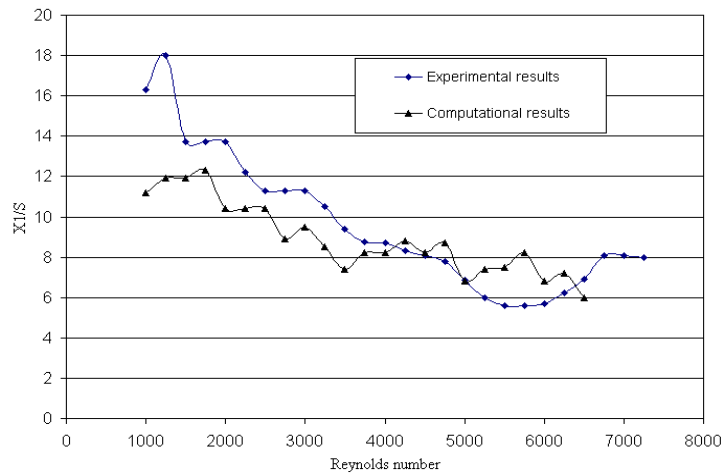


Figure 11. Comparison of experimental and computational X_1 reattachment length for $Re > 1000$ (laminar flow modeling method).

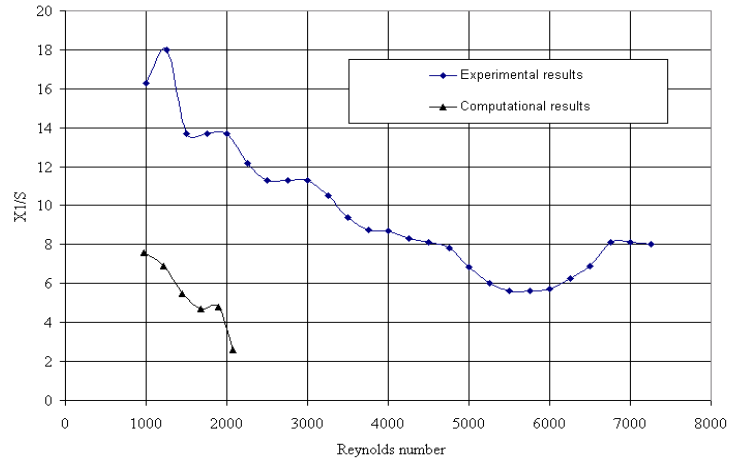


Figure 12. Comparison of experimental and computational X_1 reattachment length for low Reynolds number (Lam-Premhorst modeling method).

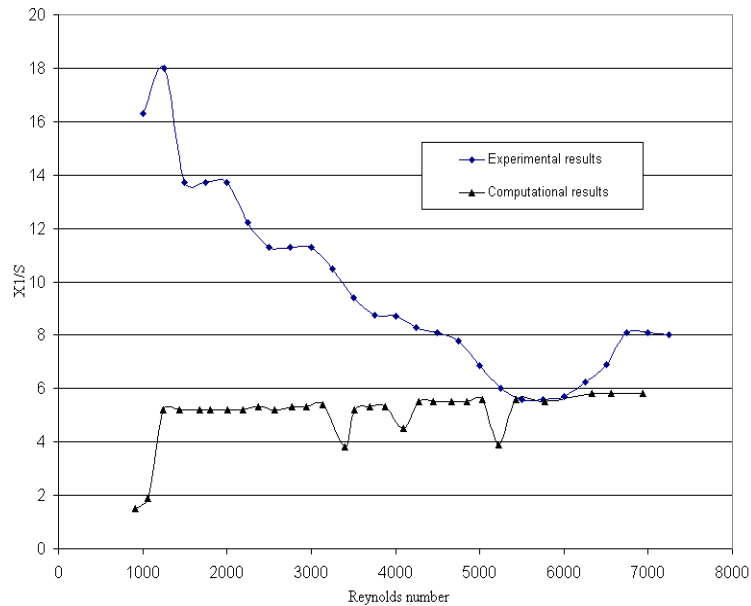


Figure 13. Comparison of experimental and computational X_1 reattachment for low Reynolds number (Launder-Sharma modeling method).

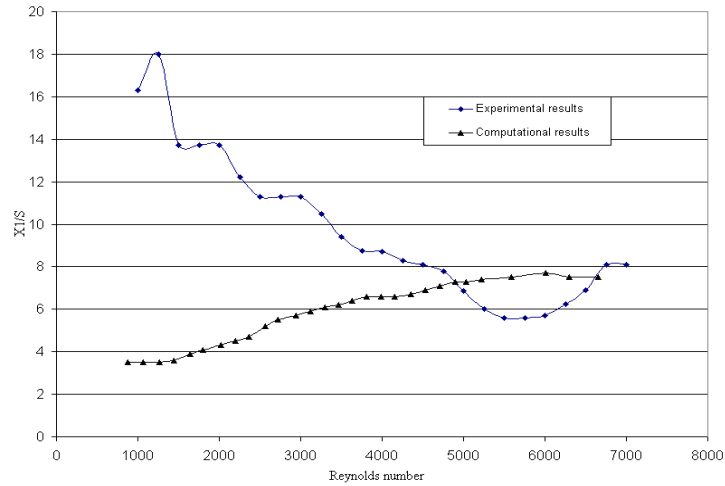


Figure 14. Comparison of experimental and computational X1 reattachment length for RNG k-ε modeling method.

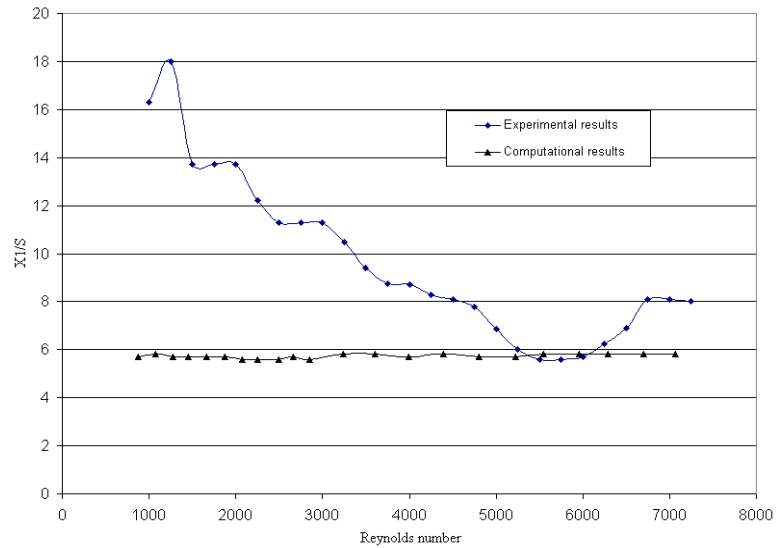


Figure 15. Comparison of experimental and computational X1 reattachment length for RSM modeling method.

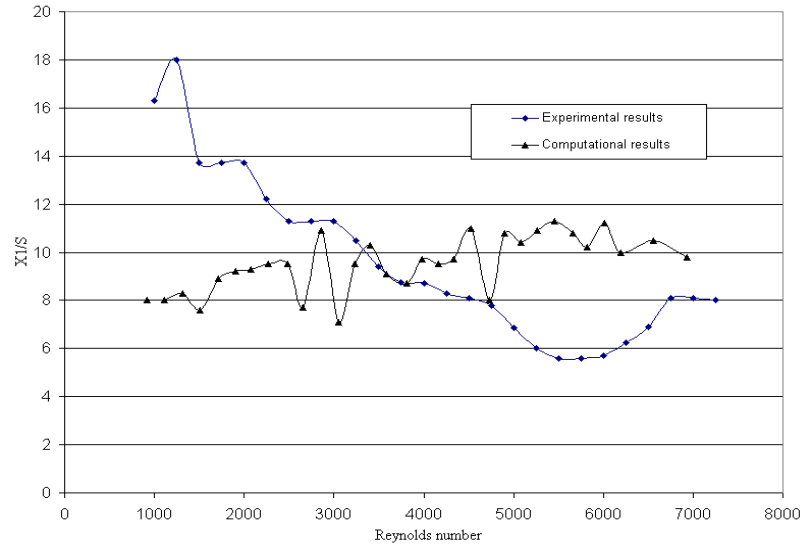


Figure 16. Comparison of experimental and computational X_1 reattachment length for standard $k-\omega$ (shear flow correction) modeling method.

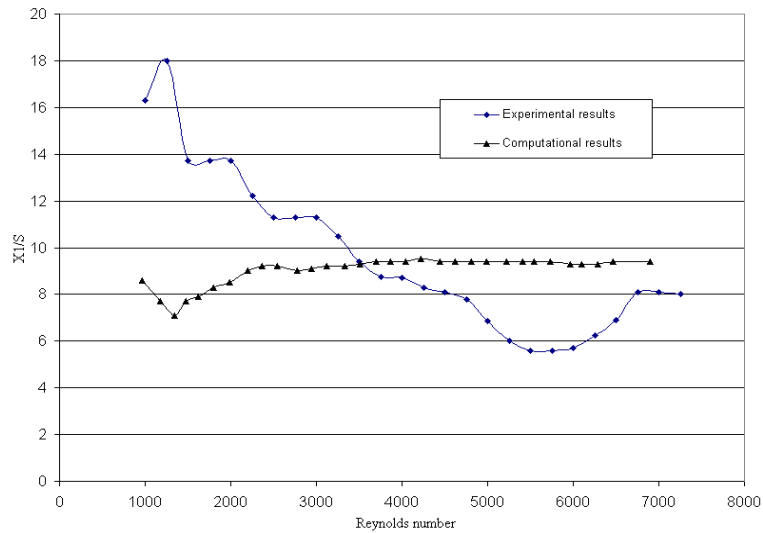


Figure 17. Comparison of experimental and computational X_1 reattachment length for standard $k-\omega$ (transitional) modeling method.

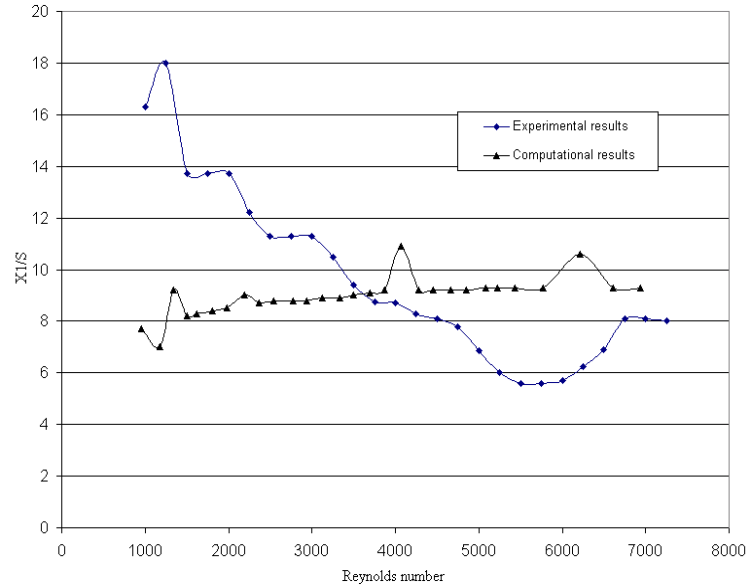


Figure 18. Comparison of experimental and computational X_1 reattachment length for SST $k-\omega$ (shear flow correction) modeling method.

At this point the study was discontinued to allow work to proceed on the principal swirling flow investigation. However, it has demonstrated that future extension of this study to expansion flow regions 2 on Fig 3.2 will not be immediately predictable by conventional 2D CFD modeling. Work carried out in parallel to this study [13] suggests that 3D turbulent modeling, even for the apparently 2D geometry, may be necessary to adequately represent the separated and recirculating flows.

4. Conclusion

Previous experimental measurements of velocity distributions and reattachment lengths of separated circulating flows downstream of a single backward-facing step in a two-dimensional channel for a Reynolds Number range of $70 < Re < 8000$ show that the length of the separation zone and reattachment lengths are function of Reynolds number, with various flow regimes characterized by typical variations of the separation length with Reynolds number (Fig .3). The conclusions that can be drawn from this preliminary study are:

- i. This is an apparently simple flow, but nevertheless it is difficult to model its features accurately. Different turbulence models give different results (Fig 11 – 18) but they contradict each other in some cases and do not match the experimental results
- ii. Grid independence in itself does not indicate that a CFD model is correct. In the same way, a similar result from different turbulent closures does not mean that a CFD model is correct.
- iii. Other work by Tasri (2005) suggests that 2D turbulent computational modelling of such flows does not predict the details of the separation and recirculation flows of the experiment, so 3D turbulent modelling for future simulation maybe required.

5. References

- [1] Armaly, B. F. et al (1983). "Experimental and Theoretical Investigation of Back-ward-Facing Step-Flow." *Journal of Fluid Mechanics*, **127**: 473-497.
- [2] Durst, F. and J. C. F. Pereira (1988). "Time-Dependent Laminar Backward-Facing Step Flow in a Two-Dimensional Duct." *Journal of Fluids Engineering ASME*, **110**: 289-296.
- [3] Hammad, K. J. et al. (2001). "Laminar Flow of a Herschel-Bulkley Fluid Over an Axisymmetric Sudden Expansion." *Journal of Fluids Engineering ASME*, **123**: 588-594.
- [4] Kaiktsis, L. et al (1991). "Onset of Three-Dimensionality, Equilibria, and Early Transition in Flow Over a Backward-Facing Step." *Journal of Fluid Mechanics*, **231**: 501-528.
- [5] Le, H. et al (1997). "Direct Numerical Simulation of Turbulent Flow Over a Backward-Facing Step." *Journal of Fluid Mechanics*, **330**: 349-374.
- [6] Williams, P. T. and A. J. Baker (1997). "Numerical Simulations of Laminar Flow Over a 3D Backward-Facing Step." *International Journal for Numerical Methods in Fluids*, **24**: 1159-1183.
- [7] Barkley, D. et al (2002). "Three-Dimensional Instability in Flow Over a Backward-Facing Step." *Journal of Fluid Mechanics*, **473**: 167-190.
- [8] Feuerstein, I. A. et al (1975). "Flow in an Abrupt Expansion as a Model for Biological Mass Transfer Experiments." *Journal of Biomechanics*, **8**: 41-51.
- [9] Guo, B. et al (2001). "Numerical Simulation of Unsteady Turbulent Flow in Axisymmetric Sudden Expansions." *Journal of Fluids Engineering ASME*, **123**: 574-587.
- [10] Hallett, W. L. H. (1988). "A Simple Model for the Critical Swirl in a Swirling Sudden Expansion Flow." *Journal of Fluids Engineering ASME*, **110**: 155-160.
- [11] Adams, E. W. et al (1984). Experiments on the Structure of Turbulent Reattaching Flow. Thermosciences Division Department of Mechanical Engineering Stanford University, California.
- [12] Fluent Inc. (2001). *Fluent 6.0 Users Guide*, Dec. 2001. 5 Vols, Fluent Inc, Lebanon NH, USA, p.10-78
- [13] Tasri, A. (2005). Accuracy of Nominally 2nd Order Unstructured Grid, CFD Codes. Ph.D. Thesis, University of Newcastle upon Tyne, Newcastle upon Tyne.